Application of fused filament fabrication 3D printing and molding to produce flexible, scaled neuron morphology models

Osama Habbal
Department of Mechanical Engineering, University of Michigan-Dearborn, Dearborn, Michigan, USA
Ahmad Farhat
Dioscuri Centre in Topological Data Analysis, Mathematical Institute, Polish Academy of Sciences, Warsaw, Poland
Reem Khalil
Department of Biology, Chemistry, and Environmental Sciences, American University of Sharjah, Sharjah, United Arab Emirates, and
Christopher Pannier
Department of Mechanical Engineering, University of Michigan-Dearborn, Dearborn, Michigan, USA

Abstract

Purpose – The purpose of this study is to assess a novel method for creating tangible three-dimensional (3D) morphologies (scaled models) of neuronal reconstructions and to evaluate its cost-effectiveness, accessibility and applicability through a classroom survey. The study addresses the challenge of accurately representing intricate and diverse dendritic structures of neurons in scaled models for educational purposes.

Design/methodology/approach – The method involves converting neuronal reconstructions from the NeuromorphoVis repository into 3D-printable mold files. An operator prints these molds using a consumer-grade desktop 3D printer with water-soluble polyvinyl alcohol filament. The molds are then filled with casting materials like polyurethane or silicone rubber, before the mold is dissolved. We tested our method on various neuron morphologies, assessing the method's effectiveness, labor, processing times and costs. Additionally, university biology students compared our 3D-printed neuron models with commercially produced counterparts through a survey, evaluating them based on their direct experience with both models.

Findings – An operator can produce a neuron morphology's initial 3D replica in about an hour of labor, excluding a one- to three-day curing period, while subsequent copies require around 30 min each. Our method provides an affordable approach to crafting tangible 3D neuron representations, presenting a viable alternative to direct 3D printing with varied material options ensuring both flexibility and durability. The created models accurately replicate the fidelity and intricacy of original computer aided design (CAD) files, making them ideal for tactile use in neuroscience education.

Originality/value – The development of data processing and cost-effective casting method for this application is novel. Compared to a previous study, this method leverages lower-cost fused filament fabrication 3D printing to create accurate physical 3D representations of neurons. By using readily available materials and a consumer-grade 3D printer, the research addresses the high cost associated with alternative direct 3D printing techniques to produce such intricate and robust models. Furthermore, the paper demonstrates the practicality of these 3D neuron models for educational purposes, making a valuable contribution to the field of neuroscience education.

Keywords Additive manufacturing, Neuronal morphologies, Fused filament fabrication, Rapid casting, Dissolvable support material, Neuroscience education,

Paper type Research paper

1. Introduction

Research advances in neuroscience have the potential to transform human and animal health and welfare. In undergraduate educational programs around the world, the need to improve neuroscience education is foundational. Recent educational tool developments in neuroscience have enhanced student comprehension by enabling students to visualize neurobiological

The current issue and full text archive of this journal is available on Emerald Insight at: **https://www.emerald.com/insight/1355-2546.htm**

Rapid Prototyping Journal
30/11 (2024) 192–204
Emerald Publishing Limited [ISSN 1355-2546]
[DOI 10.1108/RPJ-10-2023-0378]

Funding: This work is supported by grants from the Biosciences and Bioengineering Research Institute (BBRI) and Faculty Research Grant (FRG), American University of Sharjah (AUS).

Conflict of interest: The authors declare that the research was conducted in the absence of any commercial or financial relationships that could be construed as a potential conflict of interest.

Data availability statement: CAD files are attached with the following link www.printables.com/model/419589-molds-for-various-neuronal-morphologies

Received 27 October 2023
Revised 22 March 2024
Accepted 13 May 2024

phenomena with interactivity. For instance, active learning tools currently used in undergraduate neuroscience education include integrative use of 3D printing and Arduino microcontroller programing for students to build lab equipment such as a micromanipulator (Baden *et al.*, 2015); the use of 3D-printed neuron-equivalent circuits with conductive ink and passive electrical components for students to interrogate the passive properties of neural membranes (Giglia *et al.*, 2019); and the use of self-built low cost electroencephalogram (EEG) devices for cognitive science experiments (Segawa, 2019).

Advancing human understanding of how the brain encodes and computes information requires detailed examination of neuronal morphology (i.e. 3D structure). The 3D structure, as shown in Figure 1, dictates how information is processed within neurons and along neural circuits. However, textbook illustrations of neuronal morphology are typically limited to two-dimensional (2D) renderings. With advanced computer tools, a neuron's 3D structure can be accurately traced from histological sections, and the resultant digital reconstruction can be traced as a tree structure providing a morphology. Online repositories with digital reconstruction of neural morphologies already exist, including NeuroMorpho.Org (Ascoli, 2006; Ascoli *et al.*, 2007). The NeuroMorpho.Org repository contains over 200,000 microscopy-measured neuronal reconstructions as morphology files in standardized wireframe contour (SWC) file format (file ending ".SWC"). NeuroMorpho.Org has a free online 3D viewer that allows for rotation and zooming. The human brain project (HBP) neuron morphology viewer is another 3D viewer with great versatility, as it allows the user to import 3D reconstructions for viewing and editing from different sources such as NeuroMorpho.Org, the Allen Cell Types Database and the HBP morphology catalog (Newton *et al.*, 2017). Virtual 3D morphologies improve upon 2D images by allowing student interaction with the structure (e.g. rotation, panning, and scaling) on a computer screen, but additional tactile learning and understanding could be gained by student interaction with a physical morphology of the 3D structure at a morphology size of 10 cm to 50 cm.

Research in science education has shown that students gain a better comprehension of objects by interacting with high-fidelity handheld morphologies. For example, colored 3D-printed skull morphologies were found to give a statistically significant improvement in learning and comprehension for

Figure 1 Neuron components of pyramidal cell

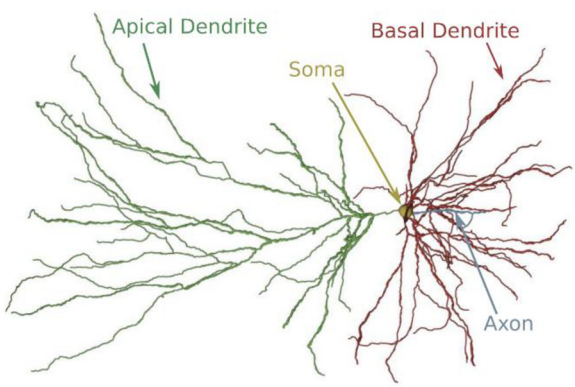

Source: Koch and Jones (2016)

medical students as compared to cadaver-sourced skulls (Chen *et al.*, 2017). Anatomical morphologies with tissue mimicking properties were successfully 3D-printed using Polyjet technique (Smith *et al.*, 2018). The authors leveraged neural networks to optimize parameters to generate the most realistic tissue features. The 3D-printed anatomical morphologies can also be generated using computed tomography (CT) images from deceased donors to enhance anatomy education in medical programs (O'Reilly *et al.*, 2016). Others have also utilized additive manufacturing techniques to enhance anatomy education with the aid of powder-based 3D printing to produce hard bones, silicone muscles, and perfusable blood vessels, resulting in accurate morphologies (Goh *et al.*, 2021).

Over the past decade, the ability to produce 3D morphologies of biological structures has been enhanced by increased availability and capability of 3D printers and 3D printing service providers. For the visualization of neuron structure, foundational computational work created printable morphology files (i.e. stereolithography [STL] files) from a database of traced neuron morphologies, which enabled 3D printing of neuron morphologies to approximately 25 cm in length (McDougal and Shepherd, 2015). The morphologies are biologically accurate in the dendritic structure but have a disproportionately increased dendrite diameter for printability, which also improves visibility and durability of the morphology. Three different professional-grade 3D printing methods were attempted (McDougal and Shepherd, 2015): selective laser sintering (SLS), wax casting and fused filament fabrication (FFF). A commercial provider made both rigid polymer morphologies and flexible polymer morphologies by SLS, and the provider produced metal morphologies by wax casting. McDougal and Shepherd used a university-operated professional-grade FFF machine to make rigid polymer morphologies with the aid dissolvable support material. They noted the limited availability of the professional grade FFF machine in the university setting at the time. Professional-grade 3D printing systems have a high capital cost (typically >$30,000) and high operating costs due to proprietary materials (powder, resin or filament), so these systems are typically available as a shared machine at a university. A neuroscience program requiring neuron morphologies for education might use a shared professional-grade 3D printing system within a university, or it may use commercial providers such as online manufacturing services that accept orders as small as a single morphology. We found that the online service provider Xometry charges a minimum cost of $30 per copy for a single neuron morphology of size 45 mm × 20 mm (i.e. volume < 5 cm^3). The high morphology cost may be a barrier for the adoption of scientific neuron morphology models for classroom instruction or on-demand tangible visualization in research work.

McDougal and Shepherd attempted to produce the 3D neuron morphologies at lower cost using a consumer-grade machine which might be found in a research lab or workshop: a desktop FFF system incapable of printing dissolvable supports. They rejected this option as too impractical due to the many non-dissolvable printing supports that required delicate manual removal. We fabricated neuron morphologies using a thermoplastic polymer and a dual extrusion FFF 3D printer with water-soluble support material printed on the second extruder. The quality and robustness of the morphology can vary with the price point of the printer, and know-how of the

user. For a consumer-grade printer built from a kit, an E3D Toolchanger (E3D, Chalgrove, Oxfordshire, UK) with multiple extrusion heads and a cost of US$2,240, the resulting morphology exhibited subpar quality and strength. Better morphology quality was obtained when using a professional-grade MakerBot Method X (MakerBot, Brooklyn, NY) that has a heated chamber and retails for US$5,000. However, the resulting morphology strength was inadequate for repeated handling. Figure 2 shows the resulting prints from both machines Therefore, there is a need to expand the capabilities of digitally producing 3D neuron morphologies using widely accessible tools such as consumer-grade 3D printers and benchtop resin casting equipment so that any university or lab can produce the morphologies of a diverse set of neuron types. This is particularly important in universities that have limited funding for educational resources.

Conventional mold-making techniques, which use subtractive machining of the cavity in the mold negative, are not well-suited to automated production of a mold of intricate neuronal structure. However, additive manufacturing (3D printing) can be used to produce an intricate negative mold in a dissolvable thermoplastic material such as polyvinyl alcohol (PVA). Researchers have used 3D-printed PVA molds in applications such as microfluidic channels (Goh and Hashimoto, 2018), biocompatible gelatin scaffolds (Nagarajan *et al.*, 2021), ceramic injection molding of parts (Wick-Joliat *et al.*, 2021) and rocket engine components (Grefen *et al.*, 2021).

To expand access to 3D printing of neuron morphologies, we introduce a method to produce neuron morphologies using a consumer-grade single-extruder FFF 3D printer, soluble filament and room-temperature castable, rigid or elastomeric materials. The contributions of this work, which builds upon a study (Ascoli *et al.*, 2007), are: developing a casting method to produce neuron morphologies at the 10- to 50-cm-length scale using a consumer-grade, single-material FFF printer for low-cost accessibility to neuron morphology 3D printing; developing a computational method for generating the 3D print file for the casting method; and comparing the production cost of the method proposed in this paper and an online manufacturing service.

Figure 2 Medium spiny morphology printed using a MakerBot Method X on the left and an E3D Toolchanger on the right using PLA filament for the neuron morphology and PVA as the support material

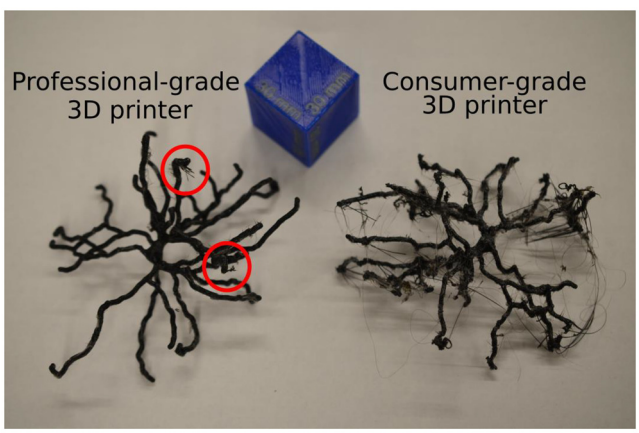

Notes: Blue 30 mm^3 cube is used for scale. Red circles highlight the smaller amount of printing errors on the morphology produced by the professional grade printer compared to the consumer-grade 3D printer
Source: Figure by authors

2. Methods

2.1 Materials

For the more rigid casts, MoldMax 60 (smooth-on, PA, USA) is used, for the medium rigidity casts, a PMC 780 WET (smooth-on, PA, USA) is used, both materials provide a compromise between flexibility and rigidity such that the resulting morphologies can resist gravity and be self-supporting. If a flexible morphology is desired, OOMOO 25 (smooth-on, PA, USA) was used, resulting in a highly flexible and stretchable morphology.

2.2 Print file preparation

The proposed method can be split into the following five parts:

1 morphology download/acquisition;
2 preprocessing in blender with the NeuromorphoVIS package;
3 computer aided design (CAD) work to generate the printable mesh file of the mold;
4 printing of the soluble mold; and
5 casting of the mold and demolding (Figure 3).

2.2.1 Morphological data retrieval

The process starts with importing the morphology file, in .SWC file extension from an online repository such as NeuroMorpho.Org [4,5]. The SWC file contains a digital representation of the neuron as a tree structure comprising points in $\mathbb{R}^3$ joined by edges. Several important properties are associated with each point, namely, its 3D spatial coordinates, its radius denoting the thickness of the branch segment at a specific 3D location, a node type indicating whether it is soma, axon or dendrite and one parent point to which it directly connects through neuronal arbors (Khalil *et al.*, 2022). It is important to note that the sample neuron morphologies that were 3D-printed in this work comprise dendrites to only reduce the overall size of the morphologies and thus axons were removed from the SWC files.

2.2.2 Preprocessing to scale arbor radii in neuron morphology

To apply modifications to the radii, the morphology .SWC file downloaded in Step (1) above is imported into blender using the NeuromorphoVIS package. The NeuromorphoVIS package is an addon to the open-source software Blender. NeuromorphoVIS manipulates and edits the neuronal reconstruction from an SWC file, converting it to an STL file format for 3D printing (Abdellah *et al.*, 2018). The NeuromorphoVIS package should be enabled in Blender to allow for manipulation of the neurons. In Blender with the NeuromorphoVIS package, under the morphology toolbox, the arbor radii are modified such that they are within the 2- to 3-mm range for ease of 3D printing in the later steps. The settings highlighted with a red box in Figure 4 have a major impact on the arbor radii. Following the diameter modifications, the structure is converted to a triangular mesh and exported as an STL (stereolithography) file.

Figure 3 Sequence of the steps involved in the proposed casting method

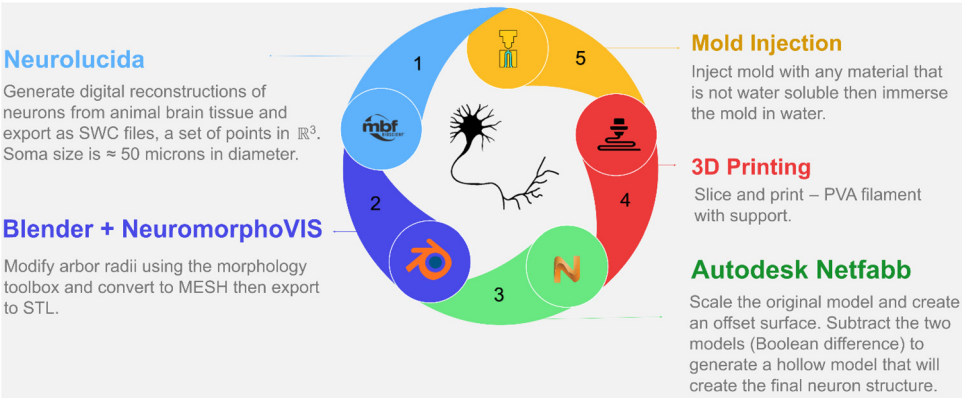

Source: Figure by authors

Figure 4 Recommended settings for printability of the neuron morphology

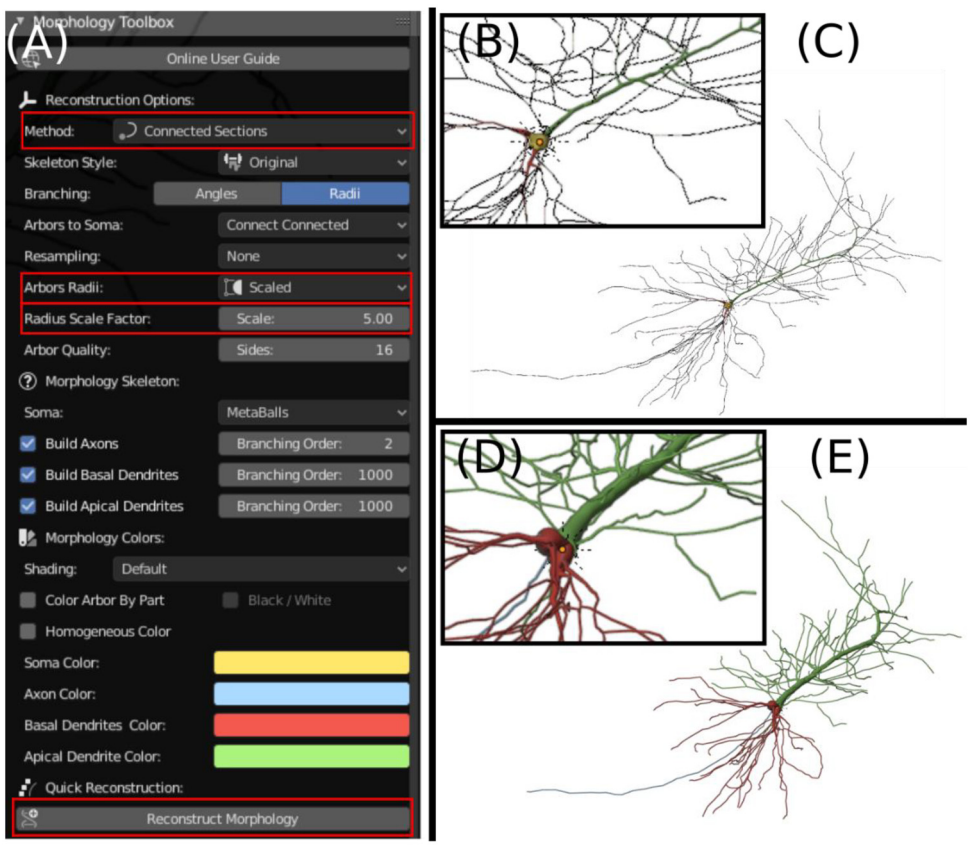

Notes: (a) Highlights the main settings of interest when modifying the neuron morphology arbor radii, (b) shows a closeup view of the "as received" neuron morphology shown in subfigure, (c) and (d) shows a closeup of the modified neuron morphology in subfigure (e) with larger radii that are more printable
Source: Figure by authors

2.2.3 Modification of mesh to generate the STL file of the mold

To create the mold structure, the STL file is imported into Autodesk Netfabb. In Netfabb, the morphology is scaled to the desired size using the scale tool; it is recommended that the maximum footprint of the scaled morphology be 80% of the 3D printer build area to ensure that the final mold is within the printable zone of the 3D printer. Following that, an offset surface is created relative to the morphology. An outer offset of 1 mm is the most suitable, as it provides adequate structure to the mold without consuming a large amount of mold material. Once the offset operation is complete, the original morphology is subtracted from the offset morphology to create the hollow channels that make up the final neuron structure.

To inject material into the mold, the mold should possess an injection hole, where the injection needle is inserted, and vent holes, from where trapped air can be released. To ensure the viscous material can be injected with relative ease into the mold, we use a 14-gauge needle, the corresponding injection hole diameter in the mold is 2.15 mm. Vent holes should be of a smaller diameter to restrict the amount of material that leaks out as the mold is fills. From trial and error, the ideal vent diameter was found to be ~0.75 mm. Diameter values depend on the printer being used, and therefore must be calibrated for each printer type. The holes can be added into the morphology using the "add perforation" tool in Netfabb. Once these steps are completed, the morphology can be exported as an STL file ready for the printing step. Figure 5 summarizes the steps for CAD work.

When working with morphologies with a high degree of branching, additional structures must be added to ensure that all the vent holes are at the same height. To achieve this, chimney-like structures called vent tubes, are added to the end of each branch, shown in Figure 6. These vent tubes are then cut to be on the same height as the build platform. Adding the vent cylinders is done in Netfabb prior to the offset step. In this process, cylinders of ~1 mm diameter are added at the termination point of each branch. Once all the branches are terminated with a tube, the tubes and the neuron morphology are combined into one body using the Boolean addition tool.

2.2.4 The soluble mold

The fourth step of the process includes slicing and printing of the generated STL file. The print material should be soluble in water.

Figure 6 Process for adding vent tubes for non-planer neuron morphologies

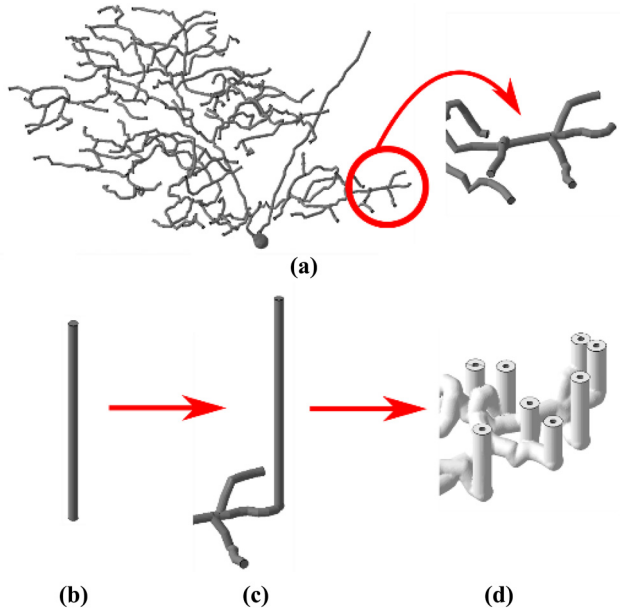

Notes: (a) Highlights the original complete morphology and specifies the region of interest, which is the termination point of the dendrites; (b) shows one vent cylinder; (c) shows a combined neuron; (d) shows the resulting mold post processing
Source: Figure by authors

From our tests, PVA filament (SainSmart) yielded useable print quality, provided it is desiccated using a food dehydrator at 40°C for 24 h prior to printing, EPVA (3DPrintLife, Southborogh, MA) was additionally tested as possible mold material, but it proved to be inadequate, due to its brittleness and fragility, making removal of the mold from the build plate and handling during injection difficult. In the slicer software of choice, the layer height should be minimized to improve quality of the final neurons. We found a layer height of 0.1 mm to be a good compromise between print quality and print time. Supports must be enabled; however,

Figure 5 Flowchart showing steps for the preparation of the mold CAD morphology

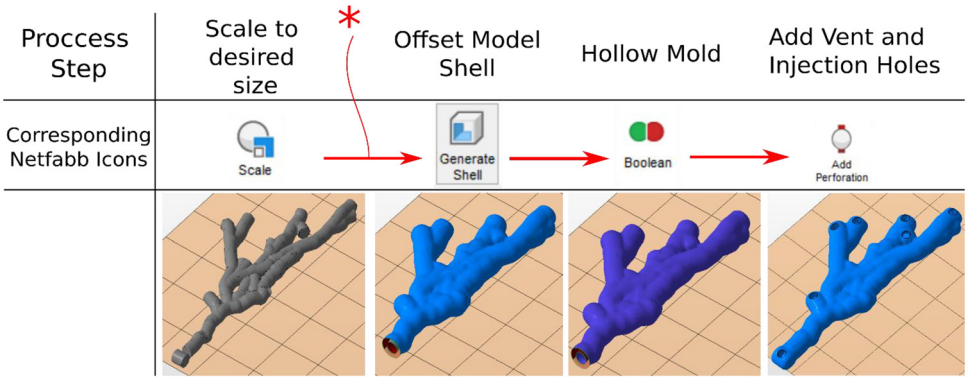

Note: The star indicates the optional step of adding vent tubes
Source: Figure by authors

care must be taken to select the support setting such that it is only from the build plate, otherwise, support structures will be placed inside of the mold, which is a region that should be free from any support structures. Moreover, travel paths of the extruder head crossing the mold channels must be minimized, such that stringing internal to the mold channels is eliminated. The print settings are summarized in Table 1.

2.2.5 Injection casting, curing and demolding

The last step of this process involves injecting the soluble mold with the casting material and applying the mold removal processing steps. The injection material can be made from any material that is flowable, does not contain water and does not dissolve in water. For ease of processing and flexibility of the final product, we selected a polyurethane and a silicone injection material. The material is prepared to the manufacturer specifications then poured into a syringe with a 14-gauge needle attached to it. It is recommended that the needle be no longer than 40 mm, to minimize required injection force. To aid in pressing the material inside the syringe during the injection process, a "press" apparatus can be made using a caulking gun and two 3D-printed adapters. The apparatus is shown in Figure 7.

Following the injection casting process, post-processing operations can begin; the mold is left to cure for a length of time that is specified by the material manufacturers – 75 min to 48 h for the materials used in this work. For demolding, the injected mold is placed in warm water, and left for 24 h to dissolve. The dissolution time can be reduced by using a heated water bath and agitation. Once dissolved, the morphology is rinsed, and any remaining mold material is removed by hand. Vent tubes are trimmed using diagonal cutting pliers along with any other excess material that might have leaked from the vent tubes and vent holes.

2.3 Method of cost analysis

The cost of each morphology neuron can be broken into the following items:

- labor cost;
- injection material cost;
- consumables (mixing cups, stir sticks, gloves);
- 3D printing filament cost; and
- lab overhead cost.

Labor costs are broken into the cost per unit time multiplied by the time required to prepare the 3D mesh, time for the injection

Table 1 Recommended print settings for printing of the soluble molds in PrusaSlicer software

Setting	Recommended value	Additional notes
Layer height	0.1 mm	0.15 to 0.2 mm is adequate for some neurons
Nozzle diameter	0.3 mm or 0.4 mm	
Support material	Enabled	Support from build plate only
Nozzle temperature	200°C	Supplier dependent
Bed temperature	60°C	Supplier dependent
Infill quality	Avoid crossing perimeters	Reduces stringing inside of the mold channels

Source: Table by authors

Figure 7 Syringe press apparatus based on a caulking gun for injecting viscous casting materials into the mold

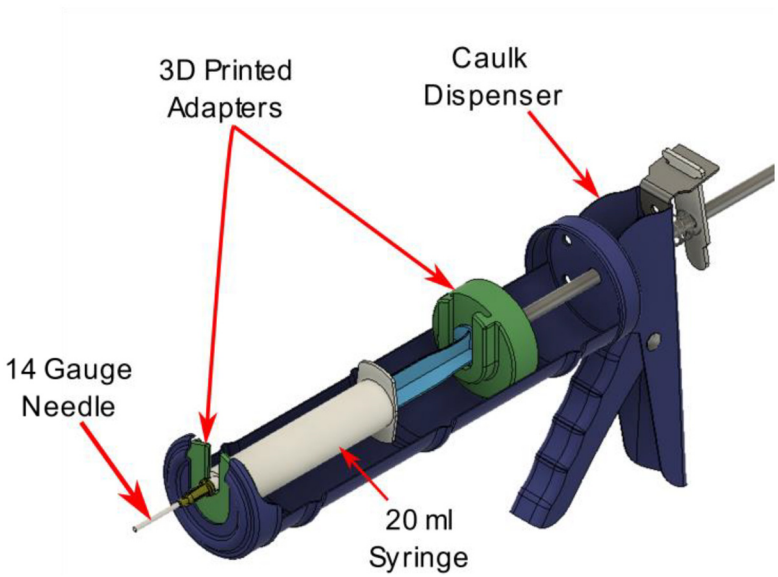

Source: Figure by authors

process and time required for post-processing operations. Injection material cost can be divided into two parts: the cost of the material used for injection and the additional cost of "wasted" material. The equation below describes the total cost for producing a neuron:

$$C_{\text{marginal}} = \left(\left(\left(\frac{t_{\text{CAD}}}{n_{\text{units}}} + t_{\text{inject}} + t_{\text{clean}} \right) \bar{c}_{\text{labor}} \right) + \left(m_{\text{elastomer}} \gamma_{\text{waste}} \bar{c}_{\text{elastomer}} \right) + c_{\text{consummable}} + m_{\text{mold}} \quad \bar{c}_{\text{mold}} \right) \gamma_{\text{overhead}}$$

where $C_{marginal}$ is the unit cost of producing neuron morphologies using the proposed method; t_{CAD} is the time required to complete the CAD work; t_{inject} is the time required to inject the mold; t_{clean} is the time required to postprocess the cured morphology; $\bar{c}_{labor}$ is the rate of labor cost; $m_{\text{melastomer}}$ is the mass required to fill the mold; γ_{waste} is the waste multiplier of the elastomer material; $\bar{c}_{elastomer}$ is the cost per kilogram of the elastomer material; $c_{consumable}$ is the cost of the injection syringes, gloves, mixing cups, mixing sticks and other molding consumables; m_{mold} is the mass of the water-soluble PVA filament required to print the mold; $\bar{c}_{mold}$ is the cost per kilogram of the PVA filament; and γ_{overhead} is the cost multiplier relating to the lab overhead.

The values for lab overhead will vary depending on the institution. Similarly, the cost of the injection material, wage rate, filament cost and the cost of the consumables will vary depending on the institution. The $_{\text{waste}}$ value is difficult value to estimate, as with care, the waste amount can be reduced. We selected a value of 1.3, as this was roughly the observed value from our tests. The overall cost will vary depending on the type, size and shape of the neuron. Complex neurons with extensive dendritic branching that require the addition of vent tubes require more time in CAD to be completed and thus, have a higher cost. Once the CAD work is completed, the cost of subsequent copies of the same neuron morphology is reduced, as it only involves the cost of the material and the casting process.

2.4 Grading 3D-printed neuron models using our method and HP Multi Jet Fusion

To evaluate the effectiveness of neurons 3D-printed with our proposed method, we conducted a classroom survey in an undergraduate Human Biology course (n = 73), requiring students to grade our models and the commercially generated ones using a HP Multi Jet Fusion 3D printer. The students were first allowed to handle and manipulate two version of a 3D-printed pyramidal neuron (HP Multi Jet Fusion and proposed method) for approximately 5 min. Immediately after handling the models, the students responded to the first part of the survey consisting of questions related to the pyramidal neurons. The same procedure was repeated with two versions of a Purkinje neuron, and students subsequently answered questions in the second part of the survey about these models. The survey questions referred to models used from our proposed method as brown neurons, and one produced by the HP Multi Jet Fusion as gray neurons, which was the color of the material of each model. The survey was administered through a Google Form whereby students were required to give consent before starting to answer the questions. The study was approved by the Institutional Review Board at the American University of Sharjah. Written informed consent was obtained from all participants. Students were informed that participation was voluntary. The consent form explained that the purpose of the study was to evaluate different 3D-printed neuron models.

There were eight five-point Likert scale questions that assessed factors such as practicality, texture, durability and clarity of anatomical details, and one that allowed students to provide qualitative feedback. The questions are summarized in Table 2.

3. Results

3.1 Fabrication of neuron morphologies by new casting method

We successfully produced neuronal morphologies by FFF 3D printing a water-soluble polymer as a casting mold and then manually injecting thermoset polymers (resins) into the molds, curing and then demolding them. We generated morphologies for a diverse set of four neuronal cell types: Purkinje NeuroMorpho.Org ID NMO_10070 (Chen *et al.*, 2013), pyramidal NeuroMorpho.Org ID NMO_86983 (Koch and Jones, 2016), medium spiny NeuroMorpho.Org ID NMO_87929 (Bicanic *et al.*, 2017) and retinal ganglion NeuroMorpho.Org ID NMO_10764 (Badea and Nathans, 2011). This diverse selection allowed us to evaluate the fabrication method with simple neuron structures (medium spiny cells) and more elaborate neuron structures (Purkinje cells). Neurons with a simple structure,

Table 2 List of questions asked in the survey

No.	Topic	Question
Q1	Texture	How would you rate the overall tactile experience of handling the neuron model?
Q2	Practicality	To what extent did the model help you understand the physical structure of a neuron?
Q3	Clarity of anatomical details	Were the dendrites of the model well-represented?
Q4	Clarity of anatomical details	Was the cell body of the model well-represented?
Q5	Durability	How durable did the neuron model feel during handling?
Q6	Clarity of anatomical details	How would you rate the accuracy of the neuron model in terms of anatomical details?
Q7	Practicality	Did handling the neuron model enhance your learning experience?
Q8	Practicality	On a scale from 1 to 5 how would you grade the neuron model overall?
Q9	Practicality	Provide any additional comments or suggestions for improving the models

Source: Table by authors

smaller number of dendrites and a planar shape remove the need for more extensive CAD preparation steps and are easier to inject and demold. The mechanical properties of the resulting neuron morphologies were varied by using three different casting materials (polyurethanes and a silicone elastomer) to obtain rigid, semi-rigid and stretchable/flexible morphologies. Figure 8 demonstrates the proposed casting method and resultant neuronal morphologies from start to end.

The resulting molded neurons inherit the surface roughness of the 3D-printed molds as shown in Figure 9. The roughness of these layer lines can be reduced by selecting a smaller layer height at the added cost of print time.

3.2 Production time requirements and cost

The time to produce each neuron morphology varied depending on the complexity, size and branching of the neurons as shown in Table 3.

The average cost of all the morphologies reproduced in this paper is compared relative to service provided morphologies that were reproduced using multiple 3D printing technologies. Figure 10 demonstrates the reduced cost of the proposed method relative to the service provided morphologies. The proposed method price reduces with each unit produced as the initial cost producing the STL print file is spread across the number of units produced, while service providers typically charge a flat rate per model.

The average cost of the neuronal examples is compared using different 3D printing methods. It can be observed from Figure 11 that the proposed casting method provides the second lowest cost per set of morphologies. The lowest production cost can be achieved with in-house direct printing of the morphologies using polylactic acid (PLA) filament and PVA filament.

Figure 9 Resulting layer lines in the final neuron morphology

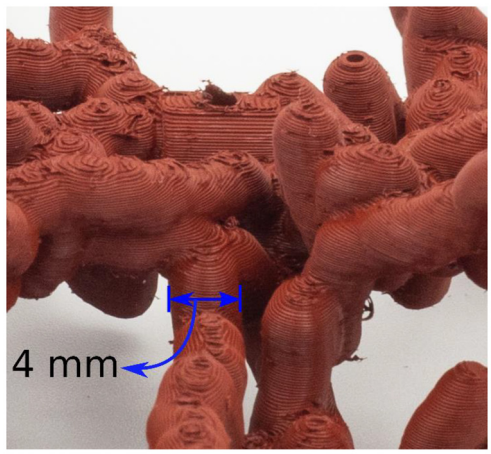

Source: Figure by authors

3.3 Assessment of neurons 3 D printed by HP Multi Jet Fusion and our method through a classroom survey

The distribution of ratings from the survey for the brown and gray models across all eight questions are presented in Figure 12. For all eight questions, the ratings were substantially higher for our models versus the HP Multi Jet Fusion models, shown in Figure 13. We conducted a series of Wilcoxon signed-rank tests to compare the characteristics of the brown and gray 3D-printed neuron models across eight attributes. Our objective was to determine if there are statistically significant differences in the tactile and visual aspects which could impact educational effectiveness. The

Figure 8 Representative neuron morphologies where (a) is ganglion cell morphology, (b) is medium spiny cell morphology, (c) is Purkinje cell morphology and (d) is pyramidal cell morphology, with different levels of complexity and sizes

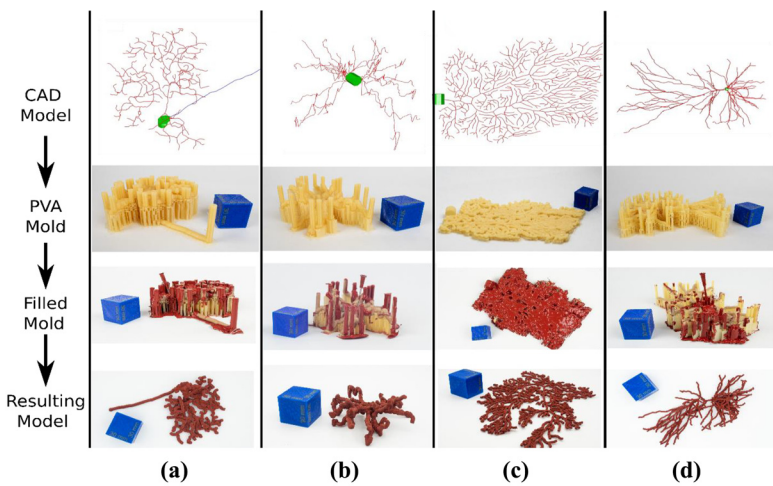

Notes: The figure captures the processing steps for each type. The first row of the figure shows the different morphologies in their raw SWC format. The second row shows the unfilled PVA soluble mold, the blue scale cube in the last 3 rows is 30 mm^3 in volume. The third row shows the filled mold prior to mold dissolution. The final row shows the post processed neuron morphologies
Source: Figure by authors

Table 3 Approximate times to produce physical copies of selected neuronal morphologies

Step	Morphology (A) (retinal ganglion cell)	Morphology (B) (medium spiny cell)	Morphology (C) (Purkinje cell)	Morphology (D) (pyramidal cell)
CAD* (labor)	0:43	0:22	00:20	00:34
Printing	11:30	11:00	36:26	16:00
Injection (labor)	00:15	00:15	00:20	00:20
Curing		1:15–48:00 (Material/temperature-dependent)		
Demolding		24:00		
Post-processing (labor)	00:10	00:10	00:15	00:10
Totals	*Morphology 1*	*Morphology 2*	*Morphology 3*	*Morphology 4*
1st copy labor steps only	1:08	00:47	00:55	1:04
Complete 1st copy	26:23–73:08	26:02–72:47	26:10–72:55	26:19–73:04
2nd copy labor steps only	00:25	00:25	00:35	00:30
Complete 2nd copy	25:40–72:25	25:40–72:25	25:50–72:35	25:45–72:30

Notes: *Manual CAD labor is not required to produce subsequent copies of a morphology. Time durations are in hh:mm format
Source: Table by authors

Figure 10 Cost comparison between the proposed casting method and the service provided morphologies cost

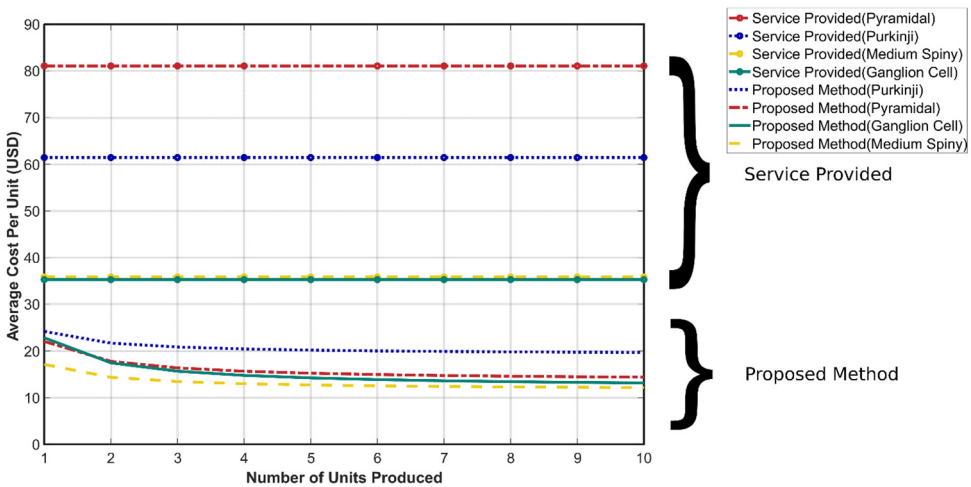

Source: Figure by authors

Figure 11 Average cost of four neuron morphologies, where (a) is ganglion cell morphology, (b) is medium spiny cell morphology, (c) is Purkinje cell morphology and (d) is pyramidal cell morphology using the proposed casting method vs. service provided morphologies

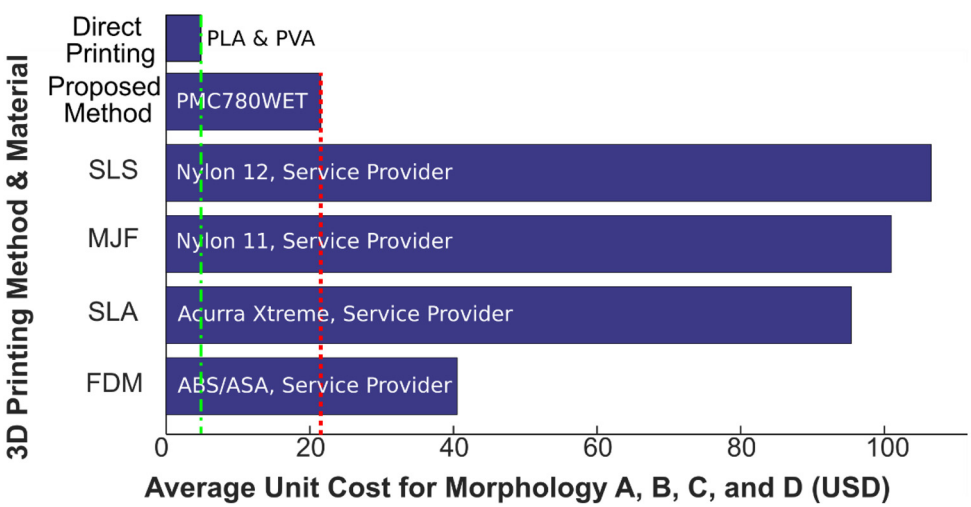

Source: Figure by authors

Figure 12 Evaluation of students' reflections on the HP Multi Jet Fusion (gray) and our proposed method (brown) 3D-printed neuron models

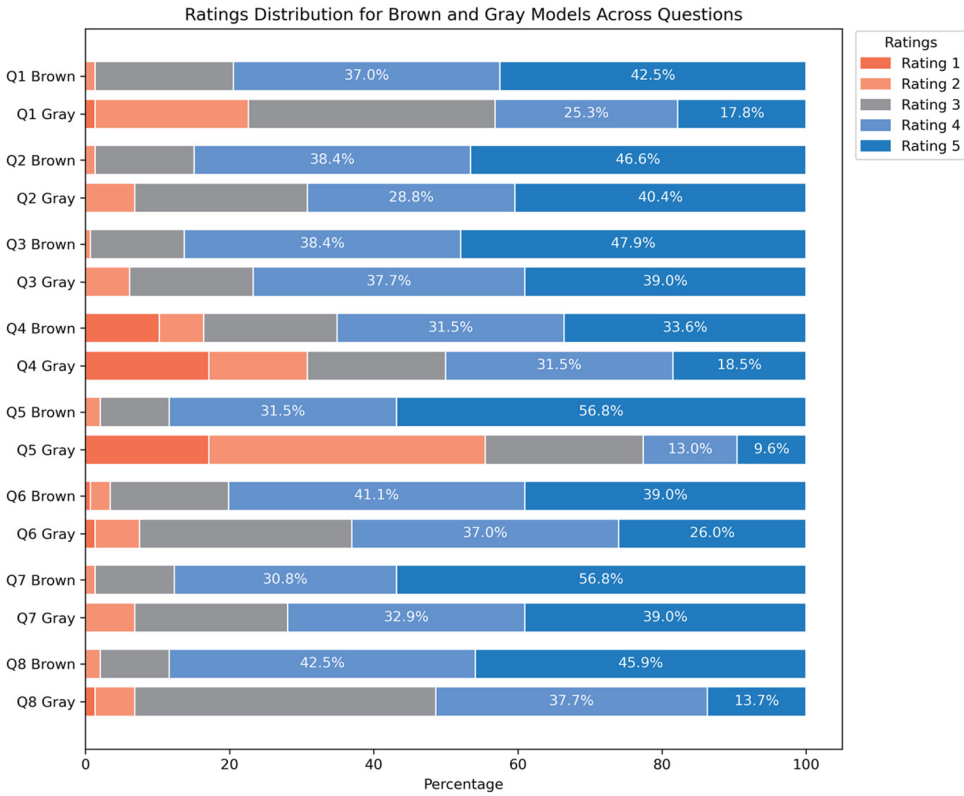

Notes: Responses of Likert scale questions for all eight questions in the survey. For each question, the top panel is the distribution of ratings for the brown model while the bottom panel is for the gray model
Source: Figure by authors

Figure 13 Representative neuron morphologies produced with HP MultiJet Fusion 3D printer where (a) is ganglion cell morphology, (b) is medium spiny cell morphology, (c) is Purkinje cell morphology and (d) is pyramidal cell morphology

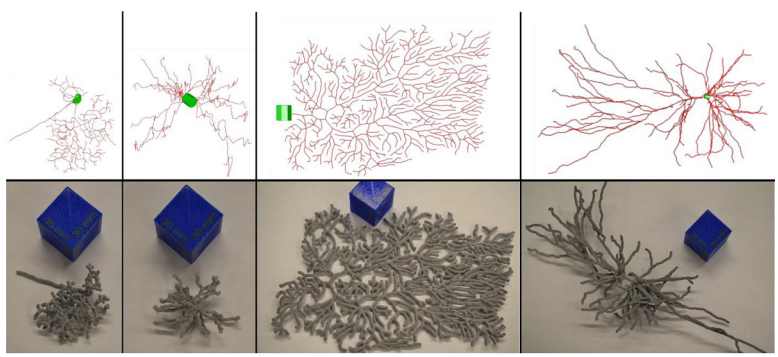

Notes: The first row of the figure shows the different morphologies in their raw SWC format, while the second shows the printed neuron morphologies. The blue cube is for scale with 30 mm^3 in volume
Source: Figure by authors

results revealed that for all eight attributes (Q1–Q8), the differences between gray and brown models were highly significant as students generally perceived the brown models to outperform the gray models (Q1: $p < 0.0001$, Q2: $p = 0.0033$, Q3: $p = 0.0083$, Q4: $p < 0.0001$, Q5: $p < 0.0001$, Q6: $p = 0.00042$, Q7 and Q8: $p < 0.0001$). For example, Q2 and Q3 both showed significant results ($p = 0.0033$ and $p = 0.0083$, respectively), suggesting that the differences in

tactile experience and visual clarity between the models are noticeable and likely to influence user preference. Similarly, Q6 and Q7 yielded p-values of $p = 0.00042$ and $p < 0.0001$, respectively, further highlighting differences in the neuron models' anatomical accuracy and handling experience.

We were also interested in optimizing our 3D-printed models and thus Q9 allowed the students to provide suggestions for improvements on both the brown and gray models. Overall, our model was perceived to be more durable, user-friendly and practical during handling, but some students preferred to color-code neuronal components for easy differentiation. As for the HP Multi Jet Fusion models, students reported that the models were too fragile and could be improved by better representing the cell body and dendrites. Collectively, the survey results indicate that student experience was generally positive with preference for our 3D-printed neurons which were considered better for educational purposes due to their durability and the ease of handling.

4. Discussion

The goal of this work is to generate neuronal morphologies that accurately reflect their 3D structure, using a cost-effective method for educational and instructional use. The use of printable 3D neuronal morphologies provides a valuable opportunity for students to interact with, manipulate and compare different neuronal morphologies. Consequently, the high-fidelity neuronal morphologies we printed in this study can nicely complement students' theoretical knowledge by enabling them to discover important morphological features that would otherwise be difficult to detect with 2D rendering. We find that the parameters used in this study to generate the sample neurons resulted in robust morphologies when handled. We predicted that our neuronal models will hold up to repeated handling and manipulation. Therefore, we evaluated the applicability of our 3D-printed neurons and compared our models with commercially produced models in a classroom setting. Students handled and inspected both models and graded each model on durability, practicality and clarity of anatomical details. The students favored our 3D-printed models as they were reported to be more durable, user-friendly and more practical to use. This suggests that the use of our 3D-printed neuron models could serve as a valuable hands-on tool in the classroom possibly enhancing theoretical knowledge of neuronal structures. Importantly, our cost-effective and simple method of producing 3D-printed neurons to engage students in the classroom enhances their accessibility.

Neural morphologies can be produced directly with the use of commercial or professional dual extrusion heads with soluble support material. The print time and print cost for such machines will be limited to the cost of the feed material and the size of the neuron morphology. Such a process can yield neural morphologies on the time scale of that is between several hours and multiple days. While this process is more user-friendly than the proposed method, its success is dependent on the following: the robustness and reliability of the dual extrusion printer used, the calibration of multiple printer parameters to ensure flawless operation and the absence of any random environmental disturbance that might cause the print to fail. The strict operational requirements on the type of 3D printer are related to the structure, fragility and size of the dendrites. However, even if the completed morphology is flawless in build, due to the layer-by-layer building technique of FFF, the strength between the layers is compromised, causing the overall structure of the morphology to be fragile and weak; not suitable for students' repeated handling. Online service providers are another method for direct printing of neuronal morphologies, they provide convenient and relatively affordable access to otherwise high-end commercial 3D printing equipment. Such commercial 3D printing systems provide a plethora of thermosets and thermoplastic polymers, metals, and ceramics as printing materials. The cost of using such services depends on a variety of factors that can include the model size, selected material, printing technology and other internal pricing mechanisms that the service provider applies. The unit price per model using the service provider is fixed, while the proposed method provides a declining cost per unit as the number of copies is increased. We used Xometery as the online service provider, the cost per model varied between $35 and $80, while the proposed method cost per model varied between $18 and $25 for the same models.

In conducting the entire process, some difficulties were faced. In the CAD stage, the addition of vent tubes to all termination points can be laborious, especially in neuron morphologies with a large number of termination points or highly random arrangement. During the slicing process, care is taken in adjusting the position of the entirety of the neuron mold in such a way that the amount of support material is minimized. In some cases, the neuron morphology has a dimension that is longer than the available build area of the 3D printer; in such a case, the morphology was split into multiple sections that can be then joined together after curing. When injecting low viscosity materials, there is a tendency for material backflow from the injection port the moment the injection needle is removed. This issue can be solved by plugging the injection hole with any object of the same diameter as the injection needle, or by simply leaving the injection needle in place if it is the highest point within the neuron morphology. During dissolution of the mold material, it be difficult to discern between what is an actual part of the neuron and what is excess material; therefore, the cleaning process must be done in a careful and slow manner as not to discard important sections of the neuron.

The proposed process is limited in several respects. A major limitation is that the maximum size of the neuron morphology is limited to the size of the build plate. This limitation can be remedied by splitting the neuron morphology into multiple prints and connecting the separate parts after injection. However, the joining process is time-consuming and difficult. The size of the neuron arbor diameter is recommended to be larger than 1 mm for most FFF 3D printers as smaller channel diameters make it difficult to push material through the syringe for injection. Similarly, the viscosity of the injection material is important; materials that have a viscosity that is thinner than water may seep through due to the porosity of the 3D-printed mold, while highly viscous materials are difficult to inject.

The viscosity of the injection material plays a key role in the success of the morphology. Materials with a mixed viscosity in

the range that is in between that of water and honey (1–1,000 cP) provide a good compromise between ease of injection and minimizing the amount of material seepage. One method for removing the visible layer lines on the resulting morphology involves injecting a 90% isopropyl alcohol solution through the unfilled PVA mold followed by a quick flush with high pressure air. This process dissolves a thin layer of material from the inner wall of the mold, thereby smoothening it. A blunt nose needle is recommended, as it allows for easy insertion into the injection hole and minimizes the chances of accidental harm to the user.

When placing vent tubes, care must be taken to ensure they do not intersect other neuron branches. Additionally, all vent holes must be placed at the same height, to avoid spillage from a low vent hole. When dissolving the mold material, warm water aids the dissolution process. We recommend leaving the PVA mold material to dissolve completely prior to handling instead of manual removal of PVA, as rough handling can tear the neuron branches. Depending on the size and complexity of the neuronal structure, the dissolution time was found to be between 24 and 48 h with multiple washout cycles. A faster dissolution time may be achievable using sonication.

Our process involves the dissolution of PVA in water, which users might dispose in sanitary sewage. An examination of the environmental impact of PVA in municipal wastewater found that municipal facilities do not sufficiently degrade the polymer, so PVA becomes an environmental contaminant to soil and land, potentially mobilizing heavy elements due to its hydrophilicity (Rolsky and Kelkar, 2021). We expect annual consumption of PVA for production of neuron morphologies to be insignificant compared to PVA consumption as protective films in laundry and dishwasher detergent pods or PVA used as a dissolvable support in other polymer 3D printing applications.

The lengthy CAD process can be reduced with the modification of NeuromorphoVIS blender package such that the processing steps are automated, making the process more user-friendly. Additionally, ready-to-print CAD morphologies can be shared through an online database, such as Printables.com, simplifying the adoption of the proposed casting method.

5. Conclusion

In conclusion, this study aimed to generate high-fidelity 3D neuronal morphologies for educational purposes using a cost-effective method. The results of this research offer valuable insights and practical implications for the field of neuroscience education. There are several advantages to integrating 3D-printed neuron models into a classroom setting using our open-source and cost-effective method. Based on the survey questions, students reported a high level of engagement and enjoyable experience while handling and manipulating our models. Neurons are inherently complex structures, so having the ability to manipulate a physical model through kinesthetic learning may enhance spatial reasoning and conceptual understanding of their morphology. There is a high potential for the use of these models in neuroscience education to facilitate active learning and engagement in students, potentially leading to improved retention of complex concepts. The fun element of actively manipulating physical structures can increase students' motivation and fuel their and curiosity in the subject. Therefore, incorporating 3D-printed neurons as educational tools in the field of neuroscience should be the standard, and it could effectively transform the way students interact with and comprehend the intricacies of neural structures, making the learning process not just informative but also inherently enjoyable.

We compared the proposed casting method with commercial dual extrusion 3D printing, as well as models produced by an online service provider using a HP MultiJet Fusion 3D printer, highlighting the strengths and weaknesses of each approach. While commercial dual extrusion 3D printing offers user-friendly and relatively quick production, it is subject to strict operational requirements and may result in fragile structures. Our research suggests that the casting method provides a viable alternative for creating robust 3D neuronal morphologies, particularly when handled by students. The online service provider approach is a convenient option for printing neuronal models. Online suppliers provide a wide array of 3D printing technologies that can produce neuronal models. We explore the cost associated with the different methods and compare it to our proposed casting method. We found that our method yielded a lower cost than the online service provider under a variety of materials and printing technologies.

However, it is important to acknowledge the limitations of the proposed casting method. The maximum size of neuron morphologies is constrained by the build plate, necessitating complex joining procedures for larger structures. Material viscosity and the dissolution process also play crucial roles in the success of this method.

As for further research, a critical area of study involves assessing the educational efficacy of 3D-printed neurons in the classroom. Investigating the impact on student learning and understanding would provide valuable insights into the effectiveness of this educational tool. Additionally, exploring alternative materials and techniques for 3D printing the mold could lead to improvements in the process.

References

Abdellah, M., Hernando, J., Eilemann, S., Lapere, S., Antille, N., Markram, H. and Schürmann, F. (2018), "NeuroMorphoVis: a collaborative framework for analysis and visualization of neuronal morphology skeletons reconstructed from microscopy stacks", *Bioinformatics*, Vol. 34 No. 13, pp. i574-i582, doi: 10.1093/bioinformatics/bty231.

Ascoli, G.A. (2006), "Mobilizing the base of neuroscience data: the case of neuronal morphologies", *Nature Reviews Neuroscience*, Vol. 7 No. 4, pp. 318-324.

Ascoli, G.A., Donohue, D.E. and Halavi, M. (2007), "NeuroMorpho.Org: a central resource for neuronal morphologies", *The Journal of Neuroscience*, Vol. 27 No. 35, pp. 9247-9245.

Badea, T.C. and Nathans, J. (2011), "Morphologies of mouse retinal ganglion cells expressing transcription factors Brn3a, Brn3b, and Brn3c: analysis of wild type and mutant cells using genetically-directed sparse labeling", *Vision Research*, Vol. 51 No. 2, pp. 269-279, doi: 10.1016/j.visres.2010.08.039.

Baden, T., Chagas, A.M., Gage, G.J., Marzullo, T.C., Prieto-Godino, L.L. and Euler, T. (2015), "Open labware: 3-D printing your own lab equipment", *PLOS Biology*, Vol. 13 No. 3, p. e1002086, doi: 10.1371/journal.pbio.1002086.

Bicanic, I., Hladnik, A. and Petanjek, Z. (2017), "A quantitative Golgi study of dendritic morphology in the mice striatal medium spiny neurons", *Frontiers in Neuroanatomy*, Vol. 11, p. 37, doi: 10.3389/fnana.2017.00037.

Chen, S., Pan, Z., Wu, Y., Gu, Z., Li, M., Liang, Z., Zhu, H., Yao, Y., Shui, W., Shen, Z., Zhao, J. and Pan, H. (2017), "The role of three-dimensional printed models of skull in anatomy education: a randomized controlled trail", *Scientific Reports*, Vol. 7 No. 1, doi: 10.1038/s41598-017-00647-1.

Chen, X.R., *et al.* (2013), "Mature Purkinje cells require the retinoic acid-related orphan receptor-α (RORα) to maintain climbing fiber Mono-innervation and other adult characteristics", *The Journal of Neuroscience*, Vol. 33 No. 22, pp. 9546-9562, doi: 10.1523/JNEUROSCI.2977-12.2013.

Giglia, G., Crisp, K., Musotto, G., Sardo, P. and Ferraro, G. (2019), "3D printing neuron equivalent circuits: an undergraduate laboratory exercise", *Journal of Undergraduate Neuroscience Education: JUNE: a Publication of FUN, Faculty for Undergraduate Neuroscience*, Vol. 18 No. 1, pp. T1-T8.

Goh, W.H. and Hashimoto, M. (2018), "Fabrication of 3D microfluidic channels and in-channel features using 3D printed, water-soluble sacrificial mold", *Macromolecular Materials and Engineering*, Vol. 303 No. 3, p. 1700484, doi: 10.1002/mame.201700484.

Goh, G.D., Sing, S.L., Lim, Y.F., Thong, J.L.J., Peh, Z.K., Mogali, S.R. and Yeong, W.Y. (2021), "Machine learning for 3D printed multi-materials tissue-mimicking anatomical morphologies", *Materials & Design*, Vol. 211, p. 110125, doi: 10.1016/j.matdes.2021.110125.

Grefen, B., Becker, J., Linke, S. and Stoll, E. (2021), "Design, production and evaluation of 3D-printed mold geometries for a hybrid rocket engine", *Aerospace*, Vol. 8 No. 8, p. 220, doi: 10.3390/aerospace8080220.

Khalil, R., Kallel, S., Farhat, A. and Dlotko, P. (2022), "Topological sholl descriptors for neuronal clustering and classification", *PLOS Computational Biology*, Vol. 18 No. 6, p. e1010229, doi: 10.1371/journal.pcbi.1010229.

Koch, C. and Jones, A. (2016), "Big science, team science, and open science for neuroscience", *Neuron*, Vol. 92 No. 3, pp. 612-616, doi: 10.1016/j.neuron.2016.10.019.

McDougal, R.A. and Shepherd, G.M. (2015), "3D-printer visualization of neuron models", *Frontiers in Neuroinformatics*, Vol. 9, doi: 10.3389/fninf.2015.00018.

Nagarajan, S., *et al.* (2021), "Sacrificial mold-assisted 3D printing of stable biocompatible gelatin scaffolds", *Bioprinting*, Vol. 22, doi: 10.1016/j.bprint.2021.e00140.

Newton, A.J.H., Seidenstein, A.H., McDougal, R.A., *et al.* (2017), "26th annual computational neuroscience meeting (CNS*2017): part 3", *BMC Neuroscience*, Vol. 18 No. S1, p. 60, doi: 10.1186/s12868-017-0372-1.

O'Reilly, M.K., Reese, S., Herlihy, T., Geoghegan, T., Cantwell, C.P., Feeney, R.N. and Jones, J.F. (2016), "Fabrication and assessment of 3D printed anatomical morphologies of the lower limb for anatomical teaching and femoral vessel access training in medicine", *Anatomical Sciences Education*, Vol. 9 No. 1, pp. 71-79, doi: 10.1002/ase.1538.

Rolsky, C. and Kelkar, V. (2021), "Degradation of polyvinyl alcohol in US wastewater treatment plants and subsequent nationwide emission estimate", *International Journal of Environmental Research and Public Health*, Vol. 18 No. 11, p. 6027, doi: 10.3390/ijerph18116027.

Segawa, J.A. (2019), "Hands-on undergraduate experiences using Low-Cost electroencephalography (EEG) devices", *Journal of Undergraduate Neuroscience Education: JUNE: a Publication of FUN, Faculty for Undergraduate Neuroscience*, Vol. 17 No. 2, pp. A119-A124.

Smith, C.F., Tollemache, N., Covill, D. and Johnston, M. (2018), "Take away body parts! An investigation into the use of 3D-printed anatomical morphologies in undergraduate anatomy education", *Anatomical Sciences Education*, Vol. 11 No. 1, pp. 44-53, doi: 10.1002/ase.1718.

Wick-Joliat, R., Tschamper, M., Kontic, R. and Penner, D. (2021), "Water-soluble sacrificial 3D printed molds for fast prototyping in ceramic injection molding", *Additive Manufacturing*, Vol. 48, p. 102408, doi: 10.1016/j.addma.2021.102408.

Corresponding author

Osama Habbal can be contacted at: ohabbal@umich.edu